

Synthesis of Sterically Demanding Secondary Phosphides and Diphosphanes and Their Utilization in Small-Molecule Activation

Jonas Bresien, Yannic Pilopp, Axel Schulz,* Lilian Sophie Szych, Alexander Villinger, and Ronald Wustrack

Cite This: <https://dx.doi.org/10.1021/acs.inorgchem.0c01934>

Read Online

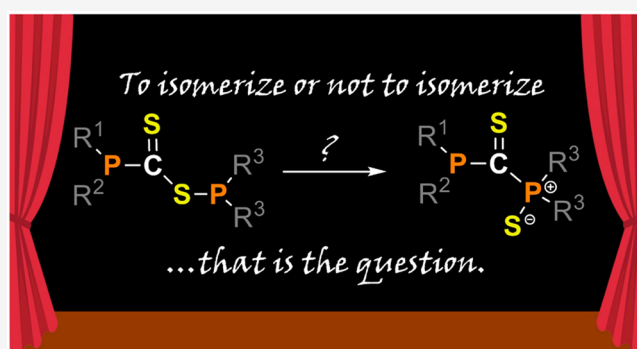
ACCESS |

Metrics & More

Article Recommendations

Supporting Information

ABSTRACT: Sterically demanding secondary potassium phosphides (4) were synthesized and investigated. Reaction with halophosphanes (5) yields diphosphanes (6), whereas reaction with CS₂ yields phosphanyl dithioformates (10). These can be further converted to the corresponding phosphanyl esters of dithioformic acid R₂P–C(S)S–PR₂ (8). One of these thioesters (8) was found to undergo a migration reaction, resulting in the formation of a phosphanylthioketone with an additional phosphanylthiolate group (9), which was used as a chiral ligand in gold coordination chemistry. The phosphanyl migration reaction was investigated by spectroscopic and theoretical methods, revealing a first-order reaction via a cyclic transition state. All species mentioned were fully characterized.

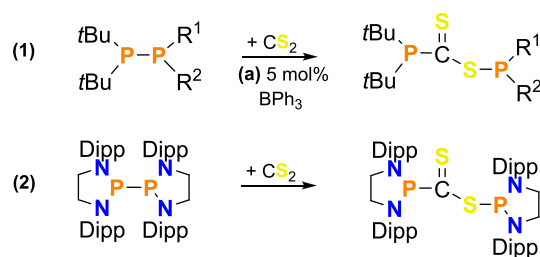


INTRODUCTION

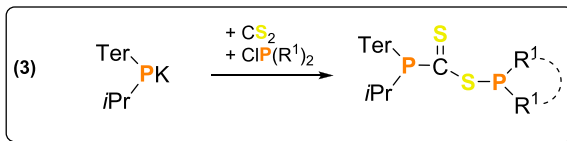
In recent years, metal-free activation of small molecules has taken on an increasingly central role in inorganic molecular chemistry. Numerous phosphorus-based compounds have proven to be of relevance in this field during the last decades.^{1–9} Of particular interest is the activation of small molecules such as CO₂ and CS₂, which can serve as building blocks for synthetic applications.^{10–19} In the past, some examples for the activation of CS₂ with phosphorus-based compounds have been published.^{20–22} We recently reported the reaction of CS₂ with phosphorus-centered biradicals, yielding bicyclic compounds,²³ and Dielmann et al. reported the activation of CS₂ by highly electron-rich tertiary phosphanes.²⁴ Furthermore, a few phosphorus-containing frustrated Lewis pairs [consisting of sterically demanding Lewis acid (LA) and Lewis base (LB)] were reported to activate CS₂, forming, e.g., adducts such as LB–C(=S)–S–LA.^{25–27} The formation of similar, rare structural motives was recently reported by Masuda et al. and Grubba et al. Conversion of diphosphanes with CS₂ yielded phosphanyl derivatives of dithioformic acid, where CS₂ is inserted between both P atoms.^{28,29} Besides the steric situation, the electronic properties of the investigated phosphanes seem to be of relevance for their reaction behavior³⁰ because this kind of reactivity has only been reported for (partially) N-substituted phosphanes (Scheme 1).

During our research on the reactivity of sterically demanding phosphorus compounds, we found that the terphenyl substituent [Ter = 2,6-bis(2,4,6-trimethylphenyl)phenyl] is a

Scheme 1. Activation of CS₂ by Phosphorus-Containing Compounds, Yielding Phosphanyl Derivatives of Dithioformic Acid^{28,29}



This Work



(1) a R¹ = R² = *i*Pr₂N; b R¹ = *i*Pr₂N; R² = Et₂N; c R¹ = R² = Et₂N;
 (2) Dipp = 2,6-diisopropylphenyl; (3) Ter = 2,6-bis-(2,4,6-trimethylphenyl)-phenyl, a R¹ = *i*Pr; b R¹ = Ph; c R¹ = *t*Bu; d P(R¹)₂ = 1,3-di-*tert*-butyl-2-chloro-1,3,2-diazaphospholidine

Received: June 30, 2020

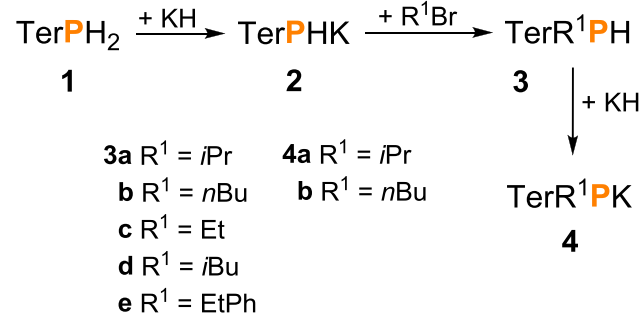
suitable ligand for stabilizing reactive bonding situations, without completely diminishing the reactivity of the stabilized species.^{31,32} Thus, this substituent is used in the course of this work.

To the best of our knowledge, no examples for the activation of CS₂ by exclusively C-substituted diphosphanes are known to date. Yet, the phosphanyl esters of dithioformic acid display interesting structural motives. Because they are potentially ambidentate ligands, binding through either S or P atoms to a metal center, these species are of interest for their use in coordination chemistry. Thus, in this work, a novel synthetic route toward arbitrarily substituted phosphanyl esters of dithioformic acid is presented. Therefore, terphenyl-stabilized phosphanyl dithioformates were synthesized, which thereafter were converted with secondary halophosphanes to form the desired R₂P–C(S)S–PR₂ species.

RESULTS AND DISCUSSION

Synthesis of Bulky Secondary Phosphides. Conversion of secondary metal phosphides with secondary halophosphanes is a well-known synthetic route to access (dissymmetric) diphosphanes. Frequently occurring side products in these syntheses are, e.g., alternative coupling products, which might be the result of in situ metal–halogen exchange reactions.^{14,33–35} For the terphenyl-stabilized phosphanes used throughout this work (1 and 3a–3e; Scheme 2), the increased

Scheme 2. Deprotonation of Terphenylphosphane 1 and Conversion to Secondary Phosphanes 3 via the Addition of Alkyl Bromides and of Secondary Phosphanes in THF, Yielding the Corresponding Potassium Phosphides 4



occurrence of various unidentified side products was noted when using lithium bases such as *n*BuLi to access the desired metal phosphides. This has been reported previously for sterically demanding phosphanes.^{31,36} Even variation of the reaction conditions (temperature and solvent) did not improve the selectivity. Thus, in subsequent reactions for the synthesis of metal phosphides, potassium hydride was used, for which we could observe very selective reaction behavior in terms of deprotonation and, furthermore, in terms of the reactivity of the isolated potassium phosphides.

A variety of bulky terphenyl-stabilized secondary phosphanes 3 can be synthesized by conversion of the previously reported terphenylpotassium phosphide 2^{37–39} with primary or secondary alkyl bromides (Scheme 2). The synthesis of 3c has been reported on a different route before, using nickel phosphanido complexes.⁴⁰ The desired products 3 can be isolated in good yield and purity. However, the deprotonation of sterically demanding secondary phosphanes such as 3a and 3b turned out to be quite challenging. Because the chosen base

KH is almost insoluble in typical organic solvents, complete deprotonation of 3 in tetrahydrofuran (THF) takes up to 10 days with stirring at room temperature. The resulting secondary potassium phosphides 4 are deep-red and highly air- and moisture-sensitive compounds, with the latter property indicating high nucleophilicity and basicity of the compounds. Therefore, the in situ use of 4 after decanting from excess KH was found to be advantageous. The completeness of the deprotonation reaction can easily be verified by ³¹P NMR spectroscopy. The products show singlet resonances with chemical shifts of 23.9 ppm (4a) and –23.6 ppm (4b) in THF-*d*₈.

4a can be crystallized from THF at room temperature in the form of small red crystals. 4a crystallizes in the monoclinic space group P2₁ with four formula units per cell (Figure 1).

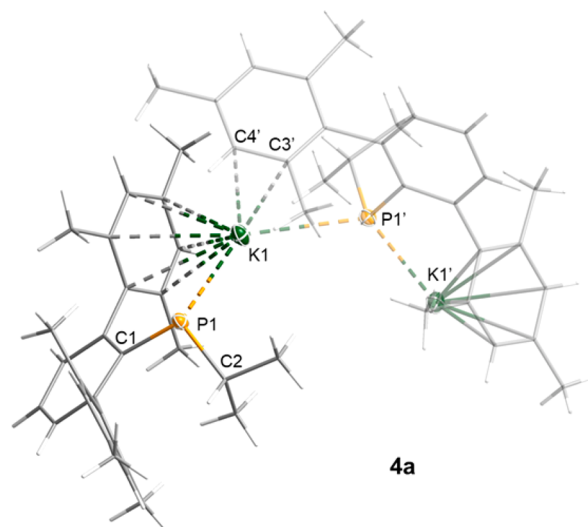


Figure 1. Molecular structure of 4a in the single crystal. Ellipsoids set at 50% probability (123 K). Selected bond length (Å) and angles (deg): P1–C1 1.847(3); P1–C2 1.887(3); K1···P1 3.2164(11); C1–P1–C2 101.92(14).

The structure in the single crystal clearly shows intramolecular coordination of K1 by the P1 atom [K1···P1 = 3.2164(11) Å; $\sum r_{\text{vdW}}(\text{K}\cdots\text{P}) = 4.55 \text{ \AA}^{41}$], as well as by the aromatic ring system of one mesityl group, which is part of the Ter substituent [average K1···C distance = 3.23 Å; $\sum r_{\text{vdW}}(\text{K}\cdots\text{C}) = 4.45 \text{ \AA}^{41}$]. Intermolecular coordination of K1 by the C3' and C4' atoms (average K1···C' distance = 3.11 Å) results in the formation of a 3D chain structure of 4a within the single crystal.

Synthesis of Diphosphanes. The investigated diphosphanes were obtained within minutes by the reaction of a stirred suspension of the previously synthesized secondary potassium phosphides 4 via the addition of secondary chlorophosphanes 5 at room temperature (Scheme 3). We isolated dissymmetric diphosphane species 6a–6h, which could be fully characterized and crystallized in the case of 6b, 6c, 6e, 6g, and 6h (Figure 2). All species were obtained in good yield, and the amount of side products formed during syntheses (3a/3b) was not significant. Diphosphane scrambling reactions yielding symmetric species were not observed. The chemical shifts of the P1 and P2 atoms within these diphosphane species are very similar in some cases. An assignment was made by means of ¹H-coupled ³¹P NMR

Scheme 3. Conversion of Secondary Potassium Phosphides with Secondary Chlorophosphanes to Diphosphanes

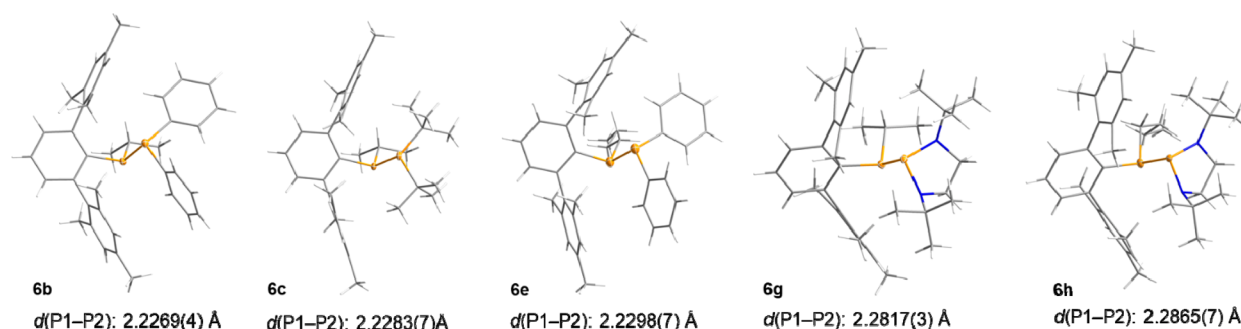
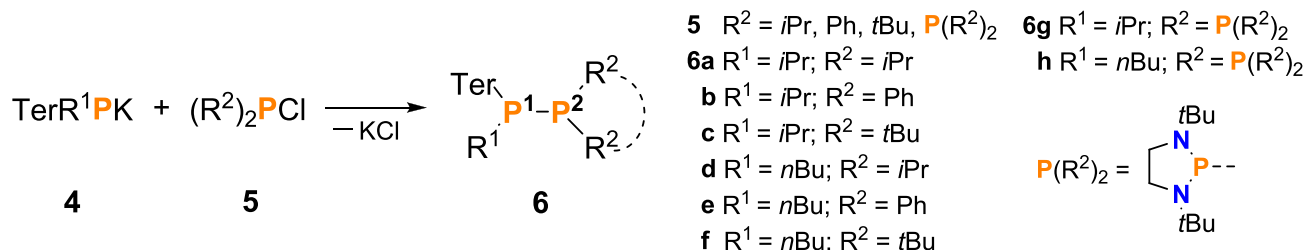


Figure 2. Molecular structures of **6b**, **6c**, **6e**, **6g**, and **6h** (from left to right) in the single crystal and the corresponding P–P bond lengths. Ellipsoids set at 50% probability (123 K; for **6e**, 173 K). Selected structural parameters and data can be found in the SI.

spectra and, if additionally required, by use of quantum-chemical calculations (Table S3). The structural parameters of **6b**, **6c**, and **6e** in the single crystal reveal that the P–P bond lengths of all C-substituted species are in the range of the sum of the covalent radii of a P–P bond [2.23 Å; cf. $\sum r_{\text{cov}}(\text{P-P}) = 2.22 \text{ \AA}$].⁴² Slightly longer P–P bonds (2.28–2.29 Å) were found for the partly N-substituted species **6g** and **6h** (Table S3). In all crystallized species, the terphenyl substituents show a noticeable deformation of the bond angles, which may be attributed to the sterically crowded situation in these diphosphanes.

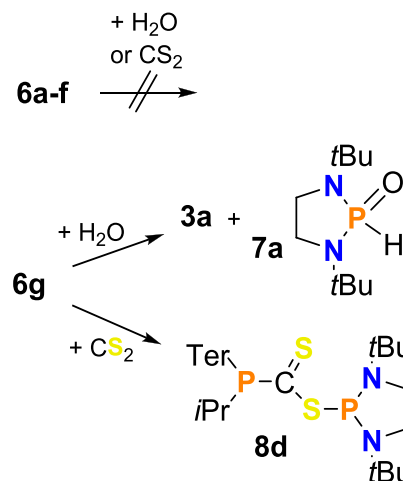
Reactivity of Diphosphanes. C-Substituted Species.

Reactivity investigations on the C-substituted diphosphanes **6a–6f** revealed that these species are stable in an aqueous benzene solution for several days at room temperature. The treatment of **6a–6f** with a large excess of CS₂ (approximately 10 equiv) did not lead to any observable reaction upon stirring for two weeks, not even under refluxing conditions.

N-Substituted Species. In contrast to the C-substituted species (vide supra), the reaction of the partly N-substituted diphosphane **6g** with water yielded the secondary phosphane **3a** and cyclic oxophosphane **7a** as products within a few hours, which could be identified via NMR spectroscopy (Scheme 4).⁴³ This reactivity is consistent with documented observations for similar species.¹⁰ The reaction of **6g** with an excess (3 equiv) of CS₂ at room temperature yielded the expected corresponding phosphanyl ester of dithioformic acid **8d**.³¹P NMR spectroscopy revealed that full conversion was reached after 2 weeks of stirring (Scheme 4). This reaction behavior of the N-substituted diphosphane **6g** toward CS₂ is in good accordance with previously reported observations.^{28,29}

The product **8d** could be isolated, fully characterized, and crystallized, and a discussion of the analytical parameters can be found below. Because the synthesis of **8** via conversion of diphosphanes with CS₂ seems to be not a universal route, we were curious to find a different synthetic approach to access

Scheme 4. Reactivity of Diphosphanes **6a–6g** toward H₂O and CS₂



these interesting species, also enabling the isolation of species in which the P1 and P2 atoms are variously substituted.

General Synthetic Route. According to our results, a stepwise synthesis of the target compound **8** starting from the potassium phosphide **4a** is indeed possible (Scheme 5).

Therefore, **4a** was reacted in the first step with CS₂ to form the bulky potassium phosphanyl dithioformate **10**. The reaction behavior of **4a** toward CS₂ is in accordance with previously reported reactions of bulky group 1 phosphides with small molecules.^{44–47}

Species **10** can be isolated in quantitative yield in the form of a pale-red, fine powder. The ³¹P NMR shift of 55.3 ppm in THF-*d*₈ is in the range of comparable compounds.^{47–49} **10** is sensitive to air and moisture but can be stored under inert-gas conditions for months.

Conversion of **10** with secondary chlorophosphanes **5** selectively afforded the desired phosphanyl esters of

Scheme 5. Synthesis of Phosphanyl Dithioformate 10a and the Subsequent Addition of 5, Yielding 8a–8d, and Migration Reaction for 8a in Solution, Resulting in the Formation of 9

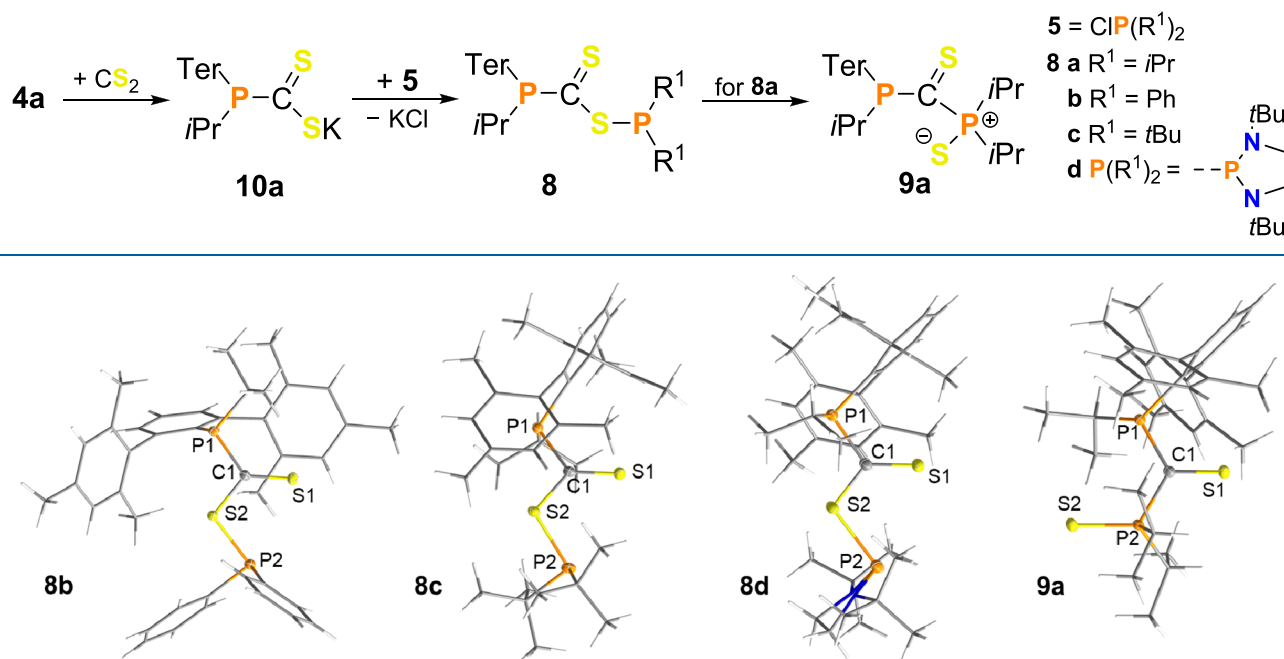


Figure 3. Molecular structures of **8b** (left), **8c** (middle left), **8d** (middle right), and **9a** (right) in the single crystal. Ellipsoids set at 50% probability (123 K). Top view on the P1–C1–S1 planes. Selected structural data are listed in Table 1.

dithioformic acid **8a–8d**. Compounds **8b–8d** can be isolated as pure, crystalline materials and were unequivocally identified by NMR spectroscopy and X-ray structure elucidation in the solid state.

This stepwise synthesis route is advantageous over the previously mentioned one starting from diphosphanes. It offers the possibility of synthesizing arbitrarily substituted species, not necessarily bearing N-substituted P atoms. Furthermore, the stepwise synthesis yielding **8d** is significantly faster than the time-consuming synthesis starting from the diphosphane **6g**. Compound **8d** can be synthesized in high purity on both synthesis routes.

Interestingly, while **8b–8d** are stable toward isomerization, **8a** directly undergoes a R_2P migration reaction within a few days of storage in solution, yielding **9a**. The migration is accompanied by a formal oxidation of one P atom from P^{III} to P^V . Because of this migration, it was impossible to fully characterize or crystallize compound **8a**. Thus, **8a** was identified by a comparison of its ^{31}P NMR signals to those of **8b–8d** and the results of theoretical calculations (Table S4). The migration product **9a** can be regarded as phosphanylthioiketone with an additional neighboring phosphanylthiolate group. To the best of our knowledge, this structural motive is unknown so far.

Heating **8b** and **8c** to 100 °C in toluene does not lead to any specific (migration) reaction: **8b** decomposes unspecifically, and **8c** is stable under these conditions.

Structure Elucidation. Compounds **8b–8d** exhibit the expected signals of the CS_2 moiety in their ^{13}C NMR spectra [**8b**: dd, 239.9 ppm, $J(^{31}P^{13}C) = 16$ and 60 Hz; **8c**: dd, 245.1 ppm, $J(^{31}P^{13}C) = 22$ and 61 Hz; **8d**: dd, 248.3 ppm, $J(^{31}P^{13}C) = 12$ and 59 Hz], as well as $C=S$ absorption bands (**8b**: 1059 cm^{-1} ; **8c**: 1072 cm^{-1} ; **8d**: 1061 cm^{-1}) in their IR spectra [see the Supporting Information (SI) for details].^{24,29}

8b–8d and **9a** could be isolated in the form of deeply colored crystals from concentrated *n*-hexane solutions at room temperature (**8b–8d**, deep red; **9a**, dark green). While **8b**, **8c**, and **9a** crystallize in monoclinic space groups (**8b** and **8c**, $P2_1/c$; **9a**, $P2_1/n$) with four formula units per unit cell, **8d** crystallizes in the triclinic space group $P\bar{1}$ with two formula units per unit cell. The most prominent structural feature of **8b–8d** is the approximately planar P1–C1(=S1)–S2 unit (Figure 3 and Table 1, dihedral angle da3). The C1–S1 bond

Table 1. Selected Structural Parameters of **8b–8d** in the Single Crystal (Figure 3)^a

parameter	8b	8c	8d
C1–S1	1.625(1)	1.624(1)	1.643(1)
S2–P2	2.1924(4)	2.1373(4)	2.3207(4)
P1–C1–S1	128.53(7)	127.94(6)	125.30(6)
S1–C1–S2	124.78(7)	126.94(6)	127.00(6)
C1–S2–P2	102.49(4)	105.44(3)	105.41(4)
da1 ^b	165.78(4)	154.66(3)	175.40(4)
da2 ^c	−19.03(8)	−23.06(7)	−5.12(9)
da3 ^d	174.1(1)	−177.2(1)	−179.4(1)

^aBond lengths in angstroms and angles in degrees. ^bda1 = $\angle P2-S2-C1-P1$ dihedral angle. ^cda2 = $\angle P2-S2-C1-S1$ dihedral angle. ^dda3 = $\angle P1-C1-S1-S2$ dihedral angle.

length in **8b–8d** are in the range of a $C=S$ bond [$\sum r_{cov}(C-S) = 1.78$ Å; $\sum r_{cov}(C=S) = 1.61$ Å].⁴² For **8b** and **8c**, the S2–P2 bond length is in the range of a single bond [$\sum r_{cov}(P-S) = 2.14$ Å; $\sum r_{cov}(P=S) = 1.96$ Å].⁴² However, the S2–P2 bond in **8d** [2.3207(4) Å, Table 1] is significantly longer than a P–S bond, probably for steric reasons.

The migration product **9a** exhibits a signal of the CS moiety at 253.7 ppm in its ^{13}C NMR spectrum [dd, $J(^{31}P^{13}C) = 24$ and 60 Hz] and a $C=S$ absorption band (983 cm^{-1}) as well as

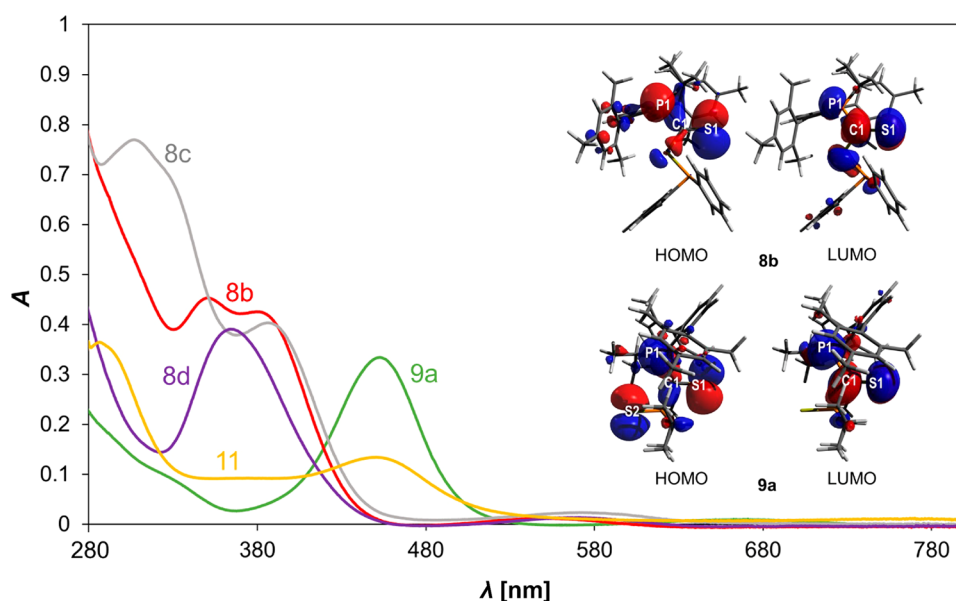


Figure 4. UV-vis spectra of **8b** ($c = 0.033 \text{ mg mL}^{-1}$, red), **8c** ($c = 0.05 \text{ mg mL}^{-1}$, gray), **8d** ($c = 0.025 \text{ mg mL}^{-1}$, purple), and **9a** ($c = 0.02 \text{ mg mL}^{-1}$, green) in hexane and **11** (vide infra, $c = 0.025 \text{ mg mL}^{-1}$, yellow) in benzene at room temperature (for absorption maxima, see Table S6). Selected Kohn-Sham orbitals (right) of **8b** (top) and **9a** (bottom). Top view on the P1-C1-S1 planes. Structures optimized at PBE0-D3/def2-SVP.

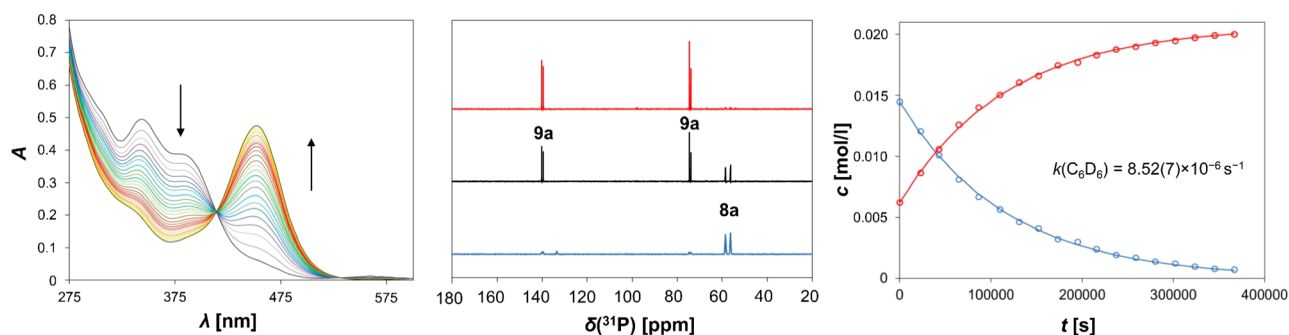


Figure 5. Left: UV-vis spectroscopic monitoring of the migration reaction from **8a** to **9a** in *n*-hexane at room temperature (time progression indicated by colors: from dark blue to yellow, with the first and last spectra depicted in black). Middle: ^{31}P NMR spectra (in C_6D_6) of the migration reaction at $t = 0 \text{ h}$ (blue), $t = 30 \text{ h}$ (black), and $t = 104 \text{ h}$ (red). Right: Migration reaction monitored by ^{31}P NMR spectroscopy in C_6D_6 (concentration of the starting material, blue; concentration of the product, red); $k_{\text{NMR},\text{benzene}} = 8.52(7) \times 10^{-6} \text{ s}^{-1}$; $k_{\text{NMR},n\text{-hexane}} = 4.75(4) \times 10^{-6} \text{ s}^{-1}$ (see the SI for further information).

a P-S absorption band (703 cm^{-1}) in its IR spectrum (see the SI for details).

In the single crystal, the migration product **9a** has a S2-P2 bond length of $1.9537(4) \text{ \AA}$, which is in the typical range for $\text{P}^{\text{V}}\text{-S}$ bonds.^{50,51} The P1-C1-S1 angle with $121.67(6)^\circ$ is comparable to the corresponding ones in compounds **8b-8d** (Figure 3).

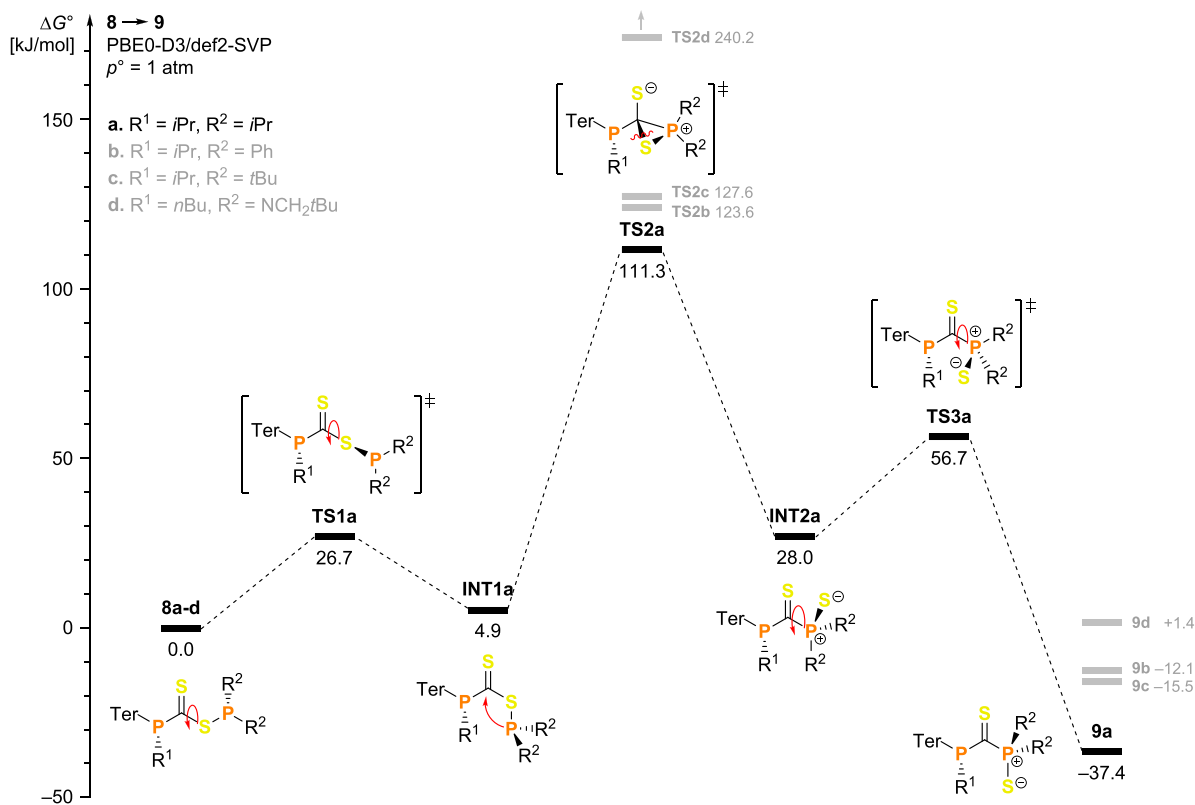
Spectroscopic Investigations on the $R_2\text{P}$ Migration Reaction. The mechanism of the migration reaction from **8a** to **9a** was investigated in detail by quantum-chemical calculations (vide infra) and also by UV-vis and NMR spectroscopy to identify a reaction mechanism and possible intermediates.

Because species **8b-8d** and **9a** are intensely colored (**8b-8d**, red/purple; **9a**, dark green), UV-vis spectra of the compounds were measured. The different absorption of the two structure types **8** and **9** in *n*-hexane is distinctly visible in the UV-vis spectra (Figure 4) of the substances. The spectrum of compound **9a** exhibits a broad and intense maximum that is centered at 453 nm (fwhm = 90 nm). Spectra

of compounds of the structure type **8** exhibit absorption maxima that are centered at smaller wavelength (between 300 and 390 nm ; see Table S6 for detailed values).

The calculated absorption maxima are in good agreement with the experimentally observed maxima (Table S6). Accordingly, the intense colors of the compounds are caused by $n \rightarrow \pi^*$ transitions [formally highest occupied molecular orbital (HOMO)-lowest unoccupied molecular orbital (LUMO) transitions; Figure 4]. For **8b** as well as for **9a**, the HOMO describes delocalized, mainly nonbonding electrons at the P1 and S1 atoms and in **9a** also at the S2 atom. In both structures, the LUMO mainly describes the π^* orbital of the C=S bond.

Because **8a** and **9a** show noticeably different absorption maxima (Table S6), it was possible to investigate the kinetics of the migration reaction using time-resolved UV-vis spectroscopy. The UV-vis spectra in *n*-hexane at room temperature clearly display the reaction progress of the migration: While the absorption maxima at $\lambda_{\text{max},1}(\mathbf{8a}) = 345 \text{ nm}$ and $\lambda_{\text{max},2}(\mathbf{8a}) = 386 \text{ nm}$ decrease, a

Scheme 6. Schematic View of the Energy Diagram (Gas Phase) of the Migration Reaction Mechanism from 8 to 9^a

^aThe intermediates for species b–d are omitted for clarity.

noticeable increase of absorption can be observed for $\lambda_{\max,1}(\mathbf{9a}) = 453 \text{ nm}$ (Figure 5). The existence of an isosbestic point at $\lambda_{\text{iso}} = 416 \text{ nm}$ indicates that, during the considered reaction period (approximately 100 h), no secondary reactions occurred (Figure 5).⁵² The migration reaction was found to be a first-order reaction at ambient temperature ($k_{\text{UV-vis}} = 4.64(1) \times 10^{-6} \text{ s}^{-1}$) with a half-life of about 42 h.

³¹P NMR spectroscopy is also well-suited to study the migration reaction because the starting material **8a** and product **9a** contain P atoms with clearly distinguishable chemical shifts (Figure 5). NMR spectroscopic investigations in *n*-hexane and C_6D_6 at room temperature could verify the first-order reaction mechanism [$k_{\text{NMR},n\text{-hexane}} = 4.75(4) \times 10^{-6} \text{ s}^{-1}$; $k_{\text{NMR},\text{benzene}} = 8.52(7) \times 10^{-6} \text{ s}^{-1}$].

The slightly different rate constants in *n*-hexane and C_6D_6 can be explained by solvent effects. Benzene stabilizes the transition state (vide infra) and therefore accelerates the migration reaction. Possible intermediates of this migration reaction could be observed by neither UV–vis nor ³¹P NMR spectroscopy, which might be due to a short lifetime or a low concentration of the intermediates in the reaction solution compared to the concentrations of the starting material and product.

Computations on the R_2P Migration Reaction. To better understand the mechanism of the migration reaction from **8a** to **9a**, computations were performed at the PBE0-D3/def2-SVP level of theory (for computational details, see also the SI).

The migration yielding **9a** is an exergonic process ($\Delta_R G^\circ = -37.4 \text{ kJ mol}^{-1}$). After rotation of the $P(iPr)_2$ moiety around the C1–S2 bond (resulting in intermediate INT1a; Scheme 6), P2 can perform a nucleophilic attack at C1. This S_N2 -type

reaction step leads to a rotamer (INT2a) of the product **9a** via cyclic transition state TS2a and is the rate-determining step (RDS) of the migration reaction. INT2a then relaxes to the final product **9a** via C–P bond rotation. Because the equilibria related to internal single-bond rotations are very fast in comparison with the RDS, the overall rate of the reaction approximately depends on the energy difference between **8** and TS2 (S86). Thus, for derivatives **8b–8d**, only transition states TS2b–TS2d were computed to estimate the reaction rates, showing larger energy differences (ΔG°) and thus slower reaction rates in agreement with the experimental observation. The agreement between experimentally estimated (*n*-hexane, 103.4 kJ mol^{-1} ; benzene, 101.9 kJ mol^{-1}) and calculated (*n*-hexane, 108.4 kJ mol^{-1} ; benzene, 107.6 kJ mol^{-1}) energy differences is reasonable. Moreover, the investigated reaction mechanism is a monomolecular reaction. Hence, it agrees with the experimentally observed reaction of first order.

As mentioned before, the migration reaction is associated with a change of the formal oxidation state of P2 from P^{III} to P^V , while the C1 atom is formally being reduced from C^{II} to C^0 . Hence, the migration process could be considered an internal redox reaction.

Coordination Chemistry of 9a. The migration product **9a** was studied as a ligand in gold coordination chemistry in order to exemplarily prove its coordination ability. It was of special interest to determine whether coordination occurs via the P and/or S atom of **9a**. Indeed, the addition of a green solution of **9a** in THF to $(SMe_2)_2AuCl$ at room temperature led to an immediate change of color to an intensely dark orange. Crystallization from *n*-hexane by slow evaporation gave complex **11** (Figure 6) in good yield. The gold complex **11**

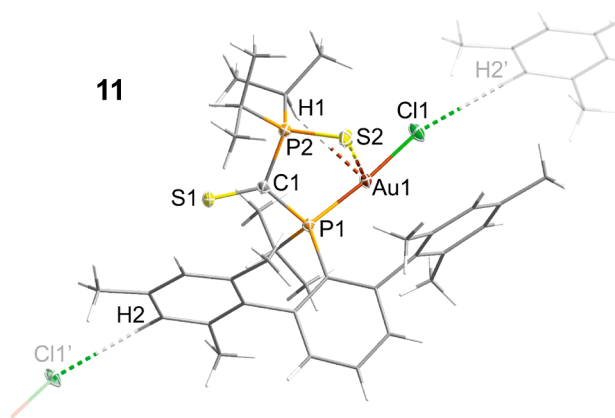


Figure 6. Molecular structure of **11** in the single crystal. Ellipsoids set at 50% probability (123 K). Selected bond length (Å) and angles (deg): P2–S2 1.9506(5); P1–Au1 2.2299(5); Cl1···H2' 2.8436(5); (C)H1···Au 2.7107(6); S2···Au1 3.3559(6); P1–Au1–Cl1 170.760(13); P1–C1–P2–S2 –41.90(7).

was fully characterized, and X-ray analysis revealed the presence of a P/S-bound AuCl complex, as depicted in Figure 6. While the P1 atom in **9a** shows an NMR shift of 139.2 ppm, it is significantly high-field-shifted to 84.6 ppm in **11**. The same phenomenon can be observed for the P2 atom (**9a**, 73.8 ppm; **11**, 40.5 ppm). **11** crystallizes in the triclinic space group $P\bar{1}$ with two formula units per cell. X-ray structure elucidation revealed a puckered five-membered Au–P–C–P–S ring exhibiting a P1–C1–P2–S2 unit in **11** that is no longer planar as in **9a** because the S2 atom is noticeably bent out of the plane [\angle P1–C1–P2–S2 dihedral angle = $-41.90(7)^\circ$]. It is well-known that gold(I) complexes tend to prefer a linear geometry, but for electronic and steric reasons, the P1–Au1–Cl1 angle in **11** is decreased to $170.76(1)^\circ$.^{53–55} Complex **11** is further stabilized by intramolecular agostic interactions: The (C)H1···Au1 bond length of 2.7107(6) Å [$\sum r_{\text{vdW}}(\text{H}\cdots\text{Au}) = 3.1 \text{ \AA}$]⁵⁶ is in the shorter range of previously reported (C)H···Au agostic interactions.^{57–60} Additionally, weak S2···Au1 interactions in **11** are indicated by a short distance of 3.3559(6) Å [$\sum r_{\text{vdW}}(\text{S}\cdots\text{Au}) = 3.5 \text{ \AA}$].⁵⁶ Intermolecular hydrogen bonding can be observed between the Cl1 atom and one *meta*-H atom of the mesityl group at the neighboring Ter substituent H2', resulting in a 3D chainlike structure in the solid state. The corresponding distance Cl1···H2' is 2.8436(5) Å [$\sum r_{\text{vdW}}(\text{H},\text{Cl}) = 3.2 \text{ \AA}$].⁵⁶ In **11**, the asymmetrically substituted P1 atom is coordinated to Au^I, which makes this type of metal complex interesting for catalytic purposes. Further investigations on the catalytic activity as well as coordination reactions of **11** are planned.

CONCLUSIONS

The findings on the reaction behavior of sterically demanding terphenyl-substituted diphosphanes are consistent with the previously published results (*vide ante*). The partly N-substituted diphosphane **6g** recently synthesized by us could be converted with CS₂, selectively yielding the phosphanyl ester of dithioformic acid. In contrast to that, the synthesized sterically demanding C-substituted diphosphanes **6a–6f** showed no reactivity toward an excess of CS₂, even under refluxing conditions, indicating that the reactions of the diphosphanes with CS₂ are kinetically forbidden.

The preparation of arbitrarily substituted phosphanyl esters of dithioformic acid **8** by a new general synthetic route is reported. This new route starts from phosphanyl dithioformates **10**, which are converted with secondary chlorophosphanes, selectively yielding the target structures.

On one occasion (R = *i*Pr), a R₂P migration within the phosphanyl ester, which is initiated by the nucleophilic attack of P2 at the C1 atom, was observed. The migration results in the formation of a phosphanylthioetone with an additional neighboring phosphanylthiolate group **9a**. Theoretical and experimental studies of the migration reaction revealed a first-order reaction with a formal three-membered cyclic transition state. Moreover, this migration process can be regarded as an internal redox process. All other studied phosphanyl esters **8** did not undergo such an isomerization process because of a larger activation barrier.

Compound **9a** further proved to be a suitable ligand for stabilization of gold(I) species, coordinating via the P and S atoms.

In future studies, other small molecules should be activated with phosphides to further investigate the properties of sterically demanding secondary potassium phosphides.

EXPERIMENTAL SECTION

All manipulations were carried out under oxygen- and moisture-free conditions under argon using standard Schlenk or drybox techniques, if not stated otherwise. All starting materials were produced using (modified) literature procedures. The reactants and solvents were obtained from commercial sources and thoroughly dried and purified. If not stated otherwise, experiments and crystallization attempts were carried out at room temperature [298(2) K]. The removal of solvents as well as evaporation of substances in vacuo was carried out at 1×10^{-3} mbar, if not stated otherwise.

Caution! KH is highly reactive and can react vigorously with air/moisture! Appropriate safety precautions should be taken (inert gas storage/handling, proper/immediate destruction of accruing excess, etc.).

Further information on the synthesis of precursors, experimental procedures, data acquisition and processing, and purification of starting materials and solvents and a full set of analytical data for each compound as well as computational details can be found in the SI.

Synthesis of Compounds. Synthesis of Secondary Phosphanes 3a–3e. Alkyl bromide [2 mmol; *i*PrBr, 0.246 g; *n*BuBr, 0.274 g; EtBr, 0.218 g; *i*BuBr, 0.274 g; 2-phenylethyl bromide (EtPhBr), 0.370 g] is added dropwise to a solution of terphenylpotassium phosphide (2 mmol, 0.768 g) in THF (15 mL). The resulting colorless suspension is stirred for 2 h. All volatile components are removed in vacuo, the remaining white solids are extracted with *n*-hexane, and the resulting suspension is filtered. The solvent of the filtrate is evaporated, yielding the product as a colorless solid. If necessary, the product can be crystallized overnight from *n*-hexane or CH₂Cl₂/CH₃CN. Yield: R¹ = *i*Pr, 95% (1.90 mmol, 0.74 g); R¹ = *n*Bu, 85% (1.70 mmol, 0.68 g); R¹ = Et, 39% (0.78 mmol, 0.29 g); R¹ = *i*Bu, 44% (0.87 mmol, 0.35 g); R¹ = EtPh, 76% (1.52 mmol, 0.69 g). **3a.** Mp: 120.0 °C. Elem anal. Calcd (found): C, 83.47 (84.59); H, 8.56 (8.79). ³¹P NMR (C₆D₆, 298.1 K, 500.13 MHz): δ –36.8 (br dd, ¹J(³¹P,¹H) = 229 Hz, J(³¹P,¹H) = 17 Hz, PH). **3b.** Mp: 110.4 °C. Elem anal. Calcd (found): C, 83.54 (83.94); H, 8.76 (8.68). ³¹P NMR (C₆D₆, 300.0 K, 101.26 MHz): δ –70.9 (d, ¹J(³¹P,¹H) = 220 Hz, PH). **3c.** Mp: 116.5 °C. Elem anal. Calcd (found): C, 84.29 (83.98); H, 7.35 (8.14). ³¹P NMR (C₆D₆, 300.0 K, 101.26 MHz): δ –63.4 (dt, ¹J(³¹P,¹H) = 220 Hz, J = 12.3 Hz, PH). **3d.** Mp: 131.2 °C. Elem anal. Calcd (found): C, 83.54 (83.05); H, 8.76 (9.31). ³¹P NMR (C₆D₆, 298.2 K, 121.51 MHz): δ –39.3 (m, ¹J(³¹P,¹H) = 219 Hz, PH), –44.3 (m, ¹J(³¹P,¹H) = 219 Hz, J(³¹P,¹H) = 20 Hz PH). **3e.** Mp: 115.2 °C. Elem anal. Calcd (found): C, 85.30 (85.42); H, 7.83 (7.94). ³¹P NMR (C₆D₆, 300.0 K, 101.26 MHz): δ –72.3 (br d, ¹J(³¹P,¹H) = 219 Hz, PH).

Synthesis of Secondary Phosphides 4a and 4b. A solution of secondary phosphane (1 mmol; *i*PrTerPH, 0.388 g; *n*BuTerPH, 0.403 g) in THF (10 mL) is added to KH (4 mmol, 0.160 g). The resulting suspension is stirred for 2 weeks, and an increase of the pressure in the flask due to hydrogen formation must be prevented using a pressure relief valve. Afterward, the solution is separated from KH by decantation, and the highly sensitive product is directly used in situ to prevent decomposition. Note: The product might still contain traces of KH, and this should be considered with respect to different substrates. The product is extremely sensitive, and the equipment needs to be thoroughly dried to prevent product decomposition. If the product should be obtained without traces of KH, the reaction mixture can be filtered in a glovebox using syringe filters (pore size: 0.45 μ m), and the solvent is evaporated under atmospheric pressure over a few days, yielding the desired product in the form of a slightly oily solid. Yield: R = *i*Pr, 80% (0.80 mmol, 0.34 g); R = *n*Bu, 83% (0.83 mmol, 0.36 g). Because of the extremely high sensitivity of the samples of **4a** and **4b**, it was not possible to obtain an accurate elemental analysis; all other analytical data as well as the reported reaction behavior prove the successful synthesis of the desired products. **4a.** Mp: 273 °C. ^{31}P NMR (THF- d_6 , 300.0 K, 101.26 MHz): δ 23.9 (m, PK). **4b.** Mp: 172 °C (dec). ^{31}P NMR (THF- d_6 , 298.5 K, 121.51 MHz): δ -23.6 (s, P).

Synthesis of Diphosphanes 6a–6f. Chlorophosphane (1 mmol; *i*Pr $_2$ PCL, 0.152 g; Ph $_2$ PCL, 0.221 g; *t*Bu $_2$ PCL, 0.181 g) is slowly added to a stirred solution of potassium phosphide (1 mmol; *i*PrTerPK, 0.426 g; *n*BuTerPK, 0.441 g) in THF (10 mL). The resulting colorless suspension is stirred for 1 h, and subsequently all volatile components are removed in vacuo. The remaining white solids are extracted with *n*-hexane, and the resulting suspension is filtered, yielding a colorless solution as the filtrate. The desired products can be crystallized overnight from a concentrated solution. Yield: R 1 = *i*Pr, R 2 = *i*Pr, 59% (0.59 mmol, 0.30 g); R 1 = *i*Pr, R 2 = Ph, 54% (0.54 mmol, 0.31 g); R 1 = *i*Pr, R 2 = *t*Bu, 48% (0.48 mmol, 0.26 g); R 1 = *n*Bu, R 2 = *i*Pr, 55% (0.55 mmol, 0.29 g); R 1 = *n*Bu, R 2 = Ph, 67% (0.67 mmol, 0.39 g); R 1 = *n*Bu, R 2 = *t*Bu: 72% (0.72 mmol, 0.39 g). **6a.** Mp: 76.6 °C. Elem anal. Calcd (found): C, 78.54 (77.79); H, 9.19 (7.79). ^{31}P NMR (C $_6$ D $_6$, 298.8 K, 121.5 MHz): δ -12.2 (d, $^1J(^{31}\text{P},^{31}\text{P})$ = 353 Hz, 1P, *i*PrTerP), 1.6 (d, $^1J(^{31}\text{P},^{31}\text{P})$ = 353 Hz, 1P, (*i*Pr) $_2$ P). **6b.** Mp: 195.6 °C. Elem anal. Calcd (found): C, 81.79 (81.34); H, 7.39 (7.81). ^{31}P NMR (C $_6$ D $_6$, 300.0 K, 101.26 MHz): δ -24.5 (br d, $^1J(^{31}\text{P},^{31}\text{P})$ = 270 Hz, 1P, (Ph) $_2$ P), -17.6 (d sep, $^1J(^{31}\text{P},^{31}\text{P})$ = 270 Hz, 1P, $J(^{31}\text{P},^1\text{H})$ = 17 Hz, *i*PrTerP). **6c.** Mp: 175.6 °C. Elem anal. Calcd (found): C, 78.91 (77.94); H, 9.46 (8.16). ^{31}P NMR (C $_6$ D $_6$, 298.2 K, 300.13 MHz): δ -1.7 (dm, $^1J(^{31}\text{P},^{31}\text{P})$ = 395 Hz, 1P, *i*PrTerP), 31.2 (dm, $^1J(^{31}\text{P},^{31}\text{P})$ = 395 Hz, 1P, (*t*Bu) $_2$ P). **6d.** Mp: 61.5 °C. Elem anal. Calcd (found): C, 78.73 (78.90); H, 9.33 (9.43). ^{31}P NMR (C $_6$ D $_6$, 300 K, 101.26 MHz): δ -37.8 (br d, $^1J(^{31}\text{P},^{31}\text{P})$ = 323 Hz, 1P, *n*BuTerP), 1.8 (dm, $^1J(^{31}\text{P},^{31}\text{P})$ = 323 Hz, 1P, (*i*Pr) $_2$ P). **6e.** Mp: 115.7 °C. Elem anal. Calcd (found): C, 81.88 (80.98); H, 7.56 (8.18). ^{31}P NMR (C $_6$ D $_6$, 300.0 K, 101.26 MHz): δ -36.2 (br d, $^1J(^{31}\text{P},^{31}\text{P})$ = 217 Hz, 1P, *n*BuTerP), -20.3 (dt, $^1J(^{31}\text{P},^{31}\text{P})$ = 217 Hz, $J(^{31}\text{P},^1\text{H})$ = 7 Hz, 1P, (Ph) $_2$ P). **6f.** Mp: 134.2 °C. Elem anal. Calcd (found): C, 79.08 (79.41); H, 9.59 (9.65). ^{31}P NMR (C $_6$ D $_6$, 300.0 K, 101.26 MHz): δ -11.4 (br d, $^1J(^{31}\text{P},^{31}\text{P})$ = 415 Hz, 1P, *n*BuTerP), 45.2 (dt, $^1J(^{31}\text{P},^{31}\text{P})$ = 415 Hz, $J(^{31}\text{P},^1\text{H})$ = 34 Hz, 1P, (*t*Bu) $_2$ P).

Synthesis of Diphosphanes 6g and 6h. A solution of potassium phosphide (1 mmol; *i*PrTerPK, 0.426 g; *n*BuTerPK, 0.441 g) in THF (10 mL) is slowly added to a stirred solution of 1,3-di-*tert*-butyl-2-chloro-1,3,2-diazaphospholidine (1 mmol, 0.237 g) in THF (3 mL). The resulting turbid yellow suspension is stirred for 1 h and filtered. The solvent of the filtrate is evaporated, the resulting white solids are extracted with CH $_2$ Cl $_2$, and insoluble components are removed by filtration. The filtrate is concentrated in vacuo, yielding crystals of the desired product. Yield: R 1 = *i*Pr, 28% (0.28 mmol, 0.17 g); R 1 = *n*Bu, 21% (0.21 mmol, 0.13 g). **6g.** Mp: 153.5 °C. Elem anal. Calcd (found): C, 75.48 (75.72); H, 9.24 (8.82); N, 4.76 (4.52). ^{31}P NMR (THF- d_6 , 298.2 K, 202.48 MHz): δ 4.7 (dm, $^1J(^{31}\text{P},^{31}\text{P})$ = 229 Hz, *i*PrTerP), 122.8 (br d, $^1J(^{31}\text{P},^{31}\text{P})$ = 229 Hz, (NCH $_2$ CH $_2$ N)P). **6h.** Mp: 124.3 °C. EA: calcd. (found) in %: C 75.71 (75.732); H 9.36

(8.349); N 4.56 (4.522). ^{31}P NMR: (THF- d_6 , 298.2 K, 121.51 MHz): δ = -26.8 (br.d, $^1J(^{31}\text{P},^{31}\text{P})$ = 213 Hz, 1P, TerPH); 121.8 (br.d, $^1J(^{31}\text{P},^{31}\text{P})$ = 213 Hz, 1P, (NCH $_2$ CH $_2$ N)P).

Synthesis of Phosphanyl Dithioformate 10a. A solution of the potassium phosphide *i*PrTerPK (1 mmol, 0.426 g) in THF (10 mL) is slowly added to a stirred excess of CS $_2$ (2 mmol, 0.152 g). The resulting orange-to-pale-red suspension is filtered to remove traces of potassium hydride from the starting material and the solvent of the filtrate evaporated, yielding the desired product in the form of a pale-red powder. Yield: 95% (0.95 mmol, 0.48 g). **10a.** Mp: 260.0 °C. Elem anal. Calcd (found): C, 66.89 (66.13); H, 6.42 (6.92); S, 12.73 (11.64). ^{31}P NMR (C $_6$ D $_6$, 299.2 K, 202.48 MHz): δ 55.3 (br d, $J(^1\text{H},^{31}\text{P})$ = 15 Hz, P).

Synthesis of Phosphanyl Esters of Dithioformic Acid 8b and 8c. The chlorophosphane CIP(R 1) $_2$ (1 mmol; CIP(Ph) $_2$, 0.221 g; CIP(*t*Bu) $_2$, 0.181 g) is added dropwise to a stirred solution of phosphanyl dithioformate (1 mmol, 0.503 g) in THF (10 mL). The resulting suspension is stirred for 10 min; afterward, the solvent is removed in vacuo. The resulting intensely colored precipitate is extracted with *n*-hexane (8 mL) and filtered. The filtrate is concentrated in vacuo, yielding a slightly viscous oily residue, from which the desired products crystallize. The supernatant is removed and discarded, and the crystals are washed with small amounts of *n*-hexane and dried in vacuo. Yield: R 1 = Ph, 53% (0.53 mmol, 0.34 g); R 1 = *t*Bu, 32.5% (0.33 mmol, 0.20 g). **8b.** Mp: 118.5 °C. Elem anal. Calcd (found): C, 74.04 (74.07); H, 6.52 (6.27); S, 9.88 (9.48). ^{31}P NMR (THF- d_6 , 297.8 K, 101.27 MHz): δ 20.7 (br d, 1P, $J(^{31}\text{P},^1\text{H})$ = 12 Hz, P(Ph) $_2$), 51.5 (m, 1P, *i*PrTerP). **8c.** Mp: 130.5 °C. Elem anal. Calcd (found): C, 71.02 (69.78); H, 8.28 (7.95); S, 10.53 (11.78). ^{31}P NMR (THF- d_6 , 298.2 K, 121.51 MHz): δ 63.8 (m, 1P, *i*PrTerP), 77.3 (m, 1P, P(*t*Bu) $_2$).

Synthesis of Phosphanyl Esters of Dithioformic Acid 8d. Method 1. A solution of potassium dithioformate [*i*PrTerPCS $_2$ K (**10a**); 1 mmol, 0.503 g) in THF (10 mL) is added slowly at 298 K to a stirred solution of 1,3-di-*tert*-butyl-2-chloro-1,3,2-diazaphospholidine (1 mmol, 0.237 g) in THF (3 mL). The resulting turbid red suspension is stirred for 10 min and subsequently filtered. The solvent of the filtrate is evaporated, the solid residue is extracted with *n*-hexane and filtered, and the filtrate is concentrated in vacuo, yielding purple crystals of the desired product overnight at 298 K. Yield: 48.0% (0.48 mmol, 0.32 g).

Method 2. CS $_2$ (3 mmol, 0.23 g) is added to a solution of diphosphane **6g** (1 mmol, 0.59 g). The resulting yellowish solution is stirred for 2 weeks, whereupon the color changes to purple. The reaction can be traced using ^{31}P NMR spectroscopy. After approximately 2 weeks, all volatile components are removed in vacuo and the resulting precipitate is solved in *n*-hexane (10 mL). The product can be crystallized overnight after removal of approximately 8 mL of the solvent in vacuo. Yield: 40.0% (0.40 mmol, 0.26 g).

8d. Mp: 182.1 °C. Elem anal. Calcd (found): C, 68.64 (69.18); H, 8.19 (8.08); N, 4.21 (4.21); S, 9.64 (9.45). ^{31}P NMR (THF- d_6 , 300.0 K, 101.26 MHz): δ 60.8 (m, 1P, *i*PrTerP), 159.9 (m, 1P, (NCH $_2$ CH $_2$ N)P).

Synthesis of the Migration Product 9a. The chlorophosphane CIP(*i*Pr) $_2$ (1 mmol, 0.153 g) is added dropwise to a stirred solution of the phosphanyl dithioformate (1 mmol, 0.503 g) in THF (10 mL). The resulting suspension is stirred for 10 min; afterward, the solvent is removed in vacuo. The solid residue is extracted with *n*-hexane (10 mL), and the resulting suspension is filtered. The filtrate is concentrated in vacuo to half of the initial volume (approximately 5 mL). After 4 days of storage, the product is obtained in the form of dark-green crystals. The supernatant is transferred into a new vessel and further concentrated, yielding equally pure crystals. Both fractions of green crystals are combined, washed with small amounts of *n*-hexane, and dried in vacuo. Yield: 31.0% (0.31 mmol, 0.18 g). **9a.** Mp: 190.8 °C. Elem anal. Calcd (found): C, 70.31 (70.34); H, 7.98 (7.85); S, 11.04 (11.11). $^{31}\text{P}\{^1\text{H}\}$ NMR (THF- d_6 , 298.1 K, 202.48 MHz): δ 73.8 (br d, $^2J(^{31}\text{P},^{31}\text{P})$ = 85 Hz, 1P, PS(*i*Pr) $_2$), 139.2 (br d, $^2J(^{31}\text{P},^{31}\text{P})$ = 85 Hz, 1P, *i*PrTerP).

Synthesis of Complex 11. **9a** (0.3 mmol, 0.171 g) is dissolved in THF (5 mL) and added dropwise to $(\text{SMe}_2)\text{AuCl}$ (0.3 mmol, 0.095 g). The resulting brownish solution is stirred for 10 min, and the solvent is removed in vacuo. The solid residue is extracted with *n*-hexane and filtered, and the filtrate is concentrated in vacuo. The product crystallizes from the concentrated solution at 5 °C in the form of small brownish crystals. Yield: 50.2% (0.14 mmol, 0.12 g). **11.** Mp: 165.8 °C. Elem anal. Calcd (found): C, 50.22 (50.32); H, 5.70 (5.53); S, 7.89 (8.07). $^{31}\text{P}\{^1\text{H}\}$ NMR (THF- d_8 , 298.2 K, 121.51 MHz): δ 40.5 (br d, $^2J(^{31}\text{P},^{31}\text{P}) = 78$ Hz, $\text{PS}(\text{iPr})_2$), 84.6 (br d, $^2J(^{31}\text{P},^{31}\text{P}) = 78$ Hz, iPrP^{Ter}).

■ ASSOCIATED CONTENT

Supporting Information

The Supporting Information is available free of charge at <https://pubs.acs.org/doi/10.1021/acs.inorgchem.0c01934>.

Experimental section, structure elucidation, syntheses of starting materials and compounds, additional spectroscopic details, spectroscopic investigations on migration reaction from **8a** to **9a**, and computational details (PDF)

Accession Codes

CCDC 2009485–2009499 contain the supplementary crystallographic data for this paper. These data can be obtained free of charge via www.ccdc.cam.ac.uk/data_request/cif, or by emailing data_request@ccdc.cam.ac.uk, or by contacting The Cambridge Crystallographic Data Centre, 12 Union Road, Cambridge CB2 1EZ, UK; fax: +44 1223 336033.

■ AUTHOR INFORMATION

Corresponding Author

Axel Schulz – Institut für Chemie, Universität Rostock, D-18059 Rostock, Germany; Leibniz-Institut für Katalyse eV an der Universität Rostock, D-18059 Rostock, Germany; orcid.org/0000-0001-9060-7065; Email: axel.schulz@uni-rostock.de

Authors

Jonas Bresien – Institut für Chemie, Universität Rostock, D-18059 Rostock, Germany; orcid.org/0000-0001-9450-3407

Yannic Pilopp – Institut für Chemie, Universität Rostock, D-18059 Rostock, Germany

Lilian Sophie Szych – Institut für Chemie, Universität Rostock, D-18059 Rostock, Germany

Alexander Villinger – Institut für Chemie, Universität Rostock, D-18059 Rostock, Germany; orcid.org/0000-0002-0868-9987

Ronald Wustrack – Institut für Chemie, Universität Rostock, D-18059 Rostock, Germany

Complete contact information is available at:

<https://pubs.acs.org/doi/10.1021/acs.inorgchem.0c01934>

Notes

The authors declare no competing financial interest.

■ ACKNOWLEDGMENTS

L.S.S. thanks the Fonds der chemischen Industrie and the Studienstiftung des deutschen Volkes for financial support and Prof. Dr. Stefanie Dehnen for helpful discussions. The University of Rostock and especially Malte Willert are acknowledged for access to the cluster computer and support with software installations.

■ REFERENCES

- (1) *The Chemistry of Organophosphorus Compounds Vol. 1: Primary, secondary and tertiary phosphines, polyphosphines and heterocyclic organophosphorus(III) compounds*; Hartley, F. R., Ed.; PATAI'S Chemistry of Functional Groups; John Wiley & Sons, Ltd.: Chichester, U.K., 1990.
- (2) *Phosphorus(III) Ligands in Homogeneous Catalysis: Design and Synthesis*; Kamer, P. C. J., van Leeuwen, P. W. N. M., Eds.; John Wiley & Sons, Ltd.: Chichester, U.K., 2012.
- (3) Welch, G. C.; Juan, R. R. S.; Masuda, J. D.; Stephan, D. W. Reversible, Metal-Free Hydrogen Activation. *Science* **2006**, *314*, 1124–1126.
- (4) *Frustrated Lewis Pairs I Uncovering and Understanding*; Erker, G., Stephan, D. W., Eds.; Topics in Current Chemistry; Springer-Verlag: Berlin, 2013; Vol. 332.
- (5) Erker, G.; Stephan, D. W. In *Frustrated Lewis Pairs II*; Erker, G., Stephan, D. W., Eds.; Topics in Current Chemistry; Springer: Berlin, 2013; Vol. 334.
- (6) Spies, P.; Erker, G.; Kehr, G.; Bergander, K.; Fröhlich, R.; Grimme, S.; Stephan, D. W. Rapid Intramolecular Heterolytic Dihydrogen Activation by a Four-Membered Heterocyclic Phosphane-Borane Adduct. *Chem. Commun.* **2007**, *2*, 5072–5074.
- (7) Lam, J.; Szkop, K. M.; Mosaferi, E.; Stephan, D. W. FLP Catalysis: Main Group Hydrogenations of Organic Unsaturated Substrates. *Chem. Soc. Rev.* **2019**, *48*, 3592–3612.
- (8) Stephan, D. W. Frustrated Lewis Pairs: A New Strategy to Small Molecule Activation and Hydrogenation Catalysis. *Dalton Trans.* **2009**, No. 17, 3129–3136.
- (9) Appelt, C.; Westenberg, H.; Bertini, F.; Ehlers, A. W.; Slootweg, J. C.; Lammertsma, K.; Uhl, W. Geminal Phosphorus/Aluminum-Based Frustrated Lewis Pairs: C-H versus $\text{C}\equiv\text{C}$ Activation and CO_2 Fixation. *Angew. Chem., Int. Ed.* **2011**, *50*, 3925–3928.
- (10) Burck, S.; Gudat, D.; Nieger, M. Diphosphanes with Polarized and Highly Reactive P-P Bonds. *Angew. Chem., Int. Ed.* **2004**, *43*, 4801–4804.
- (11) Issleib, K.; Krech, K. Alkali-Phosphorverbindungen Und Ihr Reaktives Verhalten, XXXI: Unsymmetrische Biphosphine Des Typs $\text{R}_2\text{P-PR}'_2$. *Chem. Ber.* **1965**, *98*, 1093–1096.
- (12) Burck, S.; Gudat, D.; Nieger, M.; Vinduš, D. Increasing the Lability of Polarized Phosphorus-Phosphorus Bonds. *Eur. J. Inorg. Chem.* **2008**, *2*, 704–707.
- (13) Förster, D.; Dilger, H.; Ehret, F.; Nieger, M.; Gudat, D. An Insight into the Reversible Dissociation and Chemical Reactivity of a Sterically Encumbered Diphosphane. *Eur. J. Inorg. Chem.* **2012**, *25*, 3989–3994.
- (14) Dodds, D. L.; Haddow, M. F.; Orpen, A. G.; Pringle, P. G.; Woodward, G. Stereospecific Diphosphination of Activated Acetylenes: A General Route to Backbone-Functionalized, Chelating 1,2-Diphosphinoethenes. *Organometallics* **2006**, *25*, 5937–5945.
- (15) Gudat, D. Diazaphospholenes: N-Heterocyclic Phosphines between Molecules and Lewis Pairs. *Acc. Chem. Res.* **2010**, *43*, 1307–1316.
- (16) Stephan, D. W. Frustrated Lewis Pairs: From Concept to Catalysis. *Acc. Chem. Res.* **2015**, *48*, 306–316.
- (17) Courtemanche, M. A.; Légaré, M. A.; Maron, L.; Fontaine, F. G. Reducing CO_2 to Methanol Using Frustrated Lewis Pairs: On the Mechanism of Phosphine-Borane-Mediated Hydroboration of CO_2 . *J. Am. Chem. Soc.* **2014**, *136*, 10708–10717.
- (18) Burck, S.; Hajdók, I.; Nieger, M.; Bubrin, D.; Schulze, S.; Gudat, D. Activation of Polarized Phosphorus-Phosphorus Bonds by Alkynes: Rational Synthesis of Unsymmetrical 1,2-Bisphosphine Ligands and Their Complexes. *Z. Naturforsch., B: J. Chem. Sci.* **2009**, *64b*, 63–72.
- (19) Ménard, G.; Stephan, D. W. Room Temperature Reduction of CO_2 to Methanol by Al-Based Frustrated Lewis Pairs and Ammonia Borane. *J. Am. Chem. Soc.* **2010**, *132*, 1796–1797.
- (20) Bianchini, C.; Meli, A.; Orlandini, A. Reactivity of the Triethylphosphine-Carbon Disulfide Adduct ($\text{Et}_3\text{P-CS}_2$) toward Cobalt(II) Cations in the Presence of the Tris(Tertiary Phosphines)

Triphos and Etriphos. X-Ray Crystal Structure of the Complex [(Etriphos)Co(S₂C(H)PEt₃)](BPh₄)₂. *Inorg. Chem.* **1982**, *21*, 4161–4165.

(21) Bianchini, C.; Ghilardi, C. A.; Meli, A.; Orlandini, A. Reactivity of CS₂ and Et₃P·CS₂ toward Copper(I)-Phosphine Complexes. X-Ray Crystal Structure of the Complex [(PPH₃)₂Cu(S₂CPEt₃)]BPh₄. *Inorg. Chem.* **1983**, *22*, 2188–2191.

(22) Galindo, A.; Miguel, D.; Perez, J. Phosphine-Carbon Disulfide Adducts, S₂CPR₃: Versatile Ligands in Coordination Chemistry. *Coord. Chem. Rev.* **1999**, *193–195*, 643–690.

(23) Hinz, A.; Kuzora, R.; Rosenthal, U.; Schulz, A.; Villinger, A. Activation of Small Molecules by Phosphorus Biradicaloids. *Chem. - Eur. J.* **2014**, *20*, 14659–14673.

(24) Rotering, P.; Wilm, L. F. B.; Werra, J. A.; Dielmann, F. Pyridinylidenaminophosphines: Facile Access to Highly Electron-Rich Phosphines. *Chem. - Eur. J.* **2020**, *26*, 406–411.

(25) Samigullin, K.; Georg, I.; Bolte, M.; Lerner, H. W.; Wagner, M. A Highly Reactive Geminal P/B Frustrated Lewis Pair: Expanding the Scope to C-X (X = Cl, Br) Bond Activation. *Chem. - Eur. J.* **2016**, *22*, 3478–3484.

(26) Devillard, M.; Declercq, R.; Nicolas, E.; Ehlers, A. W.; Backs, J.; Saffon-Merceron, N.; Bouhadir, G.; Slootweg, J. C.; Uhl, W.; Bourissou, D. A Significant but Constrained Geometry Pt→Al Interaction: Fixation of CO₂ and CS₂, Activation of H₂ and PhCONH₂. *J. Am. Chem. Soc.* **2016**, *138*, 4917–4926.

(27) An, K.; Zhu, J. Why Does Activation of the Weaker C = S Bond in CS₂ by P/N-Based Frustrated Lewis Pairs Require More Energy than That of the C = O Bond in CO₂? A DFT Study. *Organometallics* **2014**, *33*, 7141–7146.

(28) Giffin, N. A.; Hendsbee, A. D.; Masuda, J. D. Reactions of a Persistent Phosphinyl Radical/Diphosphine with Heteroallenes. *Dalton Trans.* **2016**, *45*, 12636–12638.

(29) Szykiewicz, N.; Ponikiewski, L.; Grubba, R. Diphosphination of CO₂ and CS₂ Mediated by Frustrated Lewis Pairs-Catalytic Route to Phosphanyl Derivatives of Formic and Dithioformic Acid. *Chem. Commun.* **2019**, *55*, 2928–2931.

(30) Blum, M.; Puntigam, O.; Plebst, S.; Ehret, F.; Bender, J.; Nieger, M.; Gudat, D. On the Energetics of P-P Bond Dissociation of Sterically Strained Tetraamino-Diphosphanes. *Dalton Trans.* **2016**, *45*, 1987–1997.

(31) Bresien, J.; Hering, C.; Schulz, A.; Villinger, A. Dimers and Trimers of Diphosphenes: A Wealth of Cyclo-Phosphanes. *Chem. - Eur. J.* **2014**, *20*, 12607–12615.

(32) Hinz, A.; Schulz, A.; Villinger, A. Synthesis of Heavy Cyclophosphadiphosphanes [CIE(μ-P-Ter)]₂ [E = P, As, Sb, or Bi; Ter = 2,6-Bis(2,4,6-Trimethylphenyl)Phenyl]. *Inorg. Chem.* **2016**, *55*, 3692–3699.

(33) Szykiewicz, N.; Ponikiewski, L.; Grubba, R. Symmetrical and Unsymmetrical Diphosphanes with Diversified Alkyl, Aryl, and Amino Substituents. *Dalton Trans.* **2018**, *47*, 16885–16894.

(34) Dodds, D. L.; Floure, J.; Garland, M.; Haddow, M. F.; Leonard, T. R.; McMullin, C. L.; Orpen, A. G.; Pringle, P. G. Diphosphanes Derived from Phobane and Phosphatrioxa-Adamantane: Similarities, Differences and Anomalies. *Dalton Trans.* **2011**, *40*, 7137–7146.

(35) Baudler, M.; Glinka, K. Monocyclic and Polycyclic Phosphanes. *Chem. Rev.* **1993**, *93*, 1623–1667.

(36) Fritz, G.; Jarmer, M.; Matern, E. Das Iso-Tetraphosphan P[P(SiMe₃)(C₆H₅)]₃. *Z. Anorg. Allg. Chem.* **1990**, *586*, 37–40.

(37) Shah, S.; Burdette, S. C.; Swavey, S.; Urbach, F. L.; Protasiewicz, J. D. Alkali Metal Induced Rupture of a Phosphorus–Phosphorus Double Bond. Electrochemical and EPR Investigations of New Sterically Protected Diphosphenes and Radical Anions [ArPPAr]•-. *Organometallics* **1997**, *16*, 3395–3400.

(38) Rabe, G. W.; Kheradmandan, S.; Yap, G. P. A. Synthesis and Structural Characterization of the Solvent-Free Potassium Derivative of a Terphenyl-Substituted Primary Phosphane: [(2,6-Dimesitylphenyl)P(H)K]₄. *Inorg. Chem.* **1998**, *37*, 6541–6543.

(39) Liddle, S. T.; Arnold, P. L. Synthesis and Characterisation of Yttrium Complexes Supported by the β-Diketimate Ligand

(ArNC(CH₃)CHC(CH₃)NAr)– (Ar = 2,6-Pri₂C₆H₃). *Dalton Trans.* **2007**, No. 30, 3305–3313.

(40) Ganushevich, Y. S.; Miluykov, V. A.; Polyancev, F. M.; Latypov, S. K.; Lönnecke, P.; Hey-Hawkins, E.; Yakhvarov, D. G.; Sinyashin, O. G. Nickel Phosphanido Hydride Complex: An Intermediate in the Hydrophosphination of Unactivated Alkenes by Primary Phosphine. *Organometallics* **2013**, *32*, 3914–3919.

(41) Mantina, M.; Chamberlin, A. C.; Valero, R.; Cramer, C. J.; Truhlar, D. G. Consistent van der Waals Radii for the Whole Main Group. *J. Phys. Chem. A* **2009**, *113*, 5806–5812.

(42) Pyykkö, P.; Atsumi, M. Molecular Double-Bond Covalent Radii for Elements Li–E112. *Chem. - Eur. J.* **2009**, *15*, 12770–12779.

(43) Ackermann, L.; Born, R. Modular Diamino- and Dioxophosphine Oxides and Chlorides as Ligands for Transition-Metal-Catalyzed C-C and C-N Couplings with Aryl Chlorides. *Angew. Chem., Int. Ed.* **2005**, *44*, 2444–2447.

(44) Xu, M.; Jupp, A. R.; Qu, Z.-W.; Stephan, D. W. Alkali Metal Species in the Reversible Activation of H₂. *Angew. Chem.* **2018**, *130*, 11216–11220.

(45) Xu, M.; Jupp, A. R.; Stephan, D. W. Acyl-Phosphide Anions via an Intermediate with Carbene Character: Reactions of K[PtBu₂] and CO. *Angew. Chem., Int. Ed.* **2019**, *58*, 3548–3552.

(46) Diemert, K.; Hahn, T.; Kuchen, W. Zur Kenntnis Des Natriumdiphenylphosphinoformats Ph₂PCOONa. *Phosphorus, Sulfur Silicon Relat. Elem.* **1991**, *60*, 287–294.

(47) Diemert, K.; Hahn, T.; Kuchen, W.; Tommes, P. Darstellung Und Reaktionen Einiger Lithiumphosphinoformate R₂PCOOLi Und RhPCOOLi -Ab Initio-Rechnungen Im System H₂PCOOH-Ph₃/CO₂. *Phosphorus, Sulfur Silicon Relat. Elem.* **1993**, *83*, 65–76.

(48) Diemert, K.; Hahn, T.; Kuchen, W. Zur Kenntnis Des Natriumdiphenylphosphinoformats Ph₂PCOONa. *Phosphorus, Sulfur Silicon Relat. Elem.* **1991**, *60*, 287–294.

(49) Ellermann, J.; Poersch, F.; Kunstmann, R.; Kramolowsky, R. Ein Salztartiger Organischer Komplex Mit Molekularem Stickstoff. *Angew. Chem.* **1969**, *81*, 183–185.

(50) Codding, P. W.; Kerr, K. A. Triphenylphosphine Sulfide. *Acta Crystallogr., Sect. B: Struct. Crystallogr. Cryst. Chem.* **1978**, *34*, 3785–3787.

(51) Shiba, R. K.; Keder, N. L.; Eckert, H. Structure of Tris(Phenylthio)Phosphine Sulfide. *Acta Crystallogr., Sect. C: Cryst. Struct. Commun.* **1992**, *48*, 1525–1527.

(52) Braslavsky, S. E. Glossary of Terms Used in Photochemistry 3rd Edition (IUPAC Recommendations 2006). *Pure Appl. Chem.* **2007**, *79*, 293–465.

(53) Akrivos, P. D.; Hadjikakou, S. K.; Karagiannidis, P.; Gdaniec, M.; Kosturkiewicz, Z. On the Molecular Structure of Gold(I) Complexes with Heterocyclic Thiones. The Structure of Bis(1,3-Thiazolidine-2-Thione) Gold(I) Chloride Hydrate. *Polyhedron* **1994**, *13*, 753–758.

(54) Räsänen, M. T.; Runeberg, N.; Klinga, M.; Nieger, M.; Bolte, M.; Pyykkö, P.; Leskelä, M.; Repo, T. Coordination of Pyridinethiols in Gold(I) Complexes. *Inorg. Chem.* **2007**, *46*, 9954–9960.

(55) Usón, R.; Laguna, A.; Laguna, M.; Jiménez, J.; Gómez, M. P.; Sainz, A.; Jones, P. G. Gold Complexes with Heterocyclic Thiones as Ligands. X-Ray Structure Determination of [Au(C₅H₃NS)₂]ClO₄. *J. Chem. Soc., Dalton Trans.* **1990**, *1*, 3457–3463.

(56) Holleman, A. F.; Wiberg, N.; Wiberg, E. *Lehrbuch der Anorganischen Chemie*, 102nd ed.; Walter de Gruyter & Co.: Berlin, 2007; Vol. 102.

(57) Ilie, A.; Raț, C. I.; Scheutzw, S.; Kiske, C.; Lux, K.; Klapötke, T. M.; Silvestru, C.; Karaghiosoff, K. Metallophilic Bonding and Agostic Interactions in Gold(I) and Silver(I) Complexes Bearing a Thiotetrazole Unit. *Inorg. Chem.* **2011**, *50*, 2675–2684.

(58) Friedrichs, S.; Jones, P. G. Secondary Interactions in Gold(I) Complexes with Thione Ligands. 2. Three Ionic Camphorsulfonates with Z' = 2 [1]. *Z. Naturforsch., B: J. Chem. Sci.* **2004**, *59*, 1429–1437.

(59) Friedrichs, S.; Jones, P. G. Secondary Interactions in Gold(I) Complexes with Thione Ligands. 2. Three Ionic Chlorides. *Z. Naturforsch., B: J. Chem. Sci.* **2004**, *59*, 49–57.

(60) Friedrichs, S.; Jones, P. G. Secondary Interactions in Gold(I) Complexes with Thione Ligands. 2. Three Ionic Camphorsulfonates with $Z' = 2$ [1]. *Z. Naturforsch., B: J. Chem. Sci.* **2004**, *59*, 793–801.